

Stability Analysis of a Concrete Arch Gravity Dam by 3D Finite Element Technique

Sougata Mukherjee, Nallasivam Kanagaraj

Civil Engineering Department, National Institute of Tehnology, Hamirpur, INDIA

e-mail: nallasivam_iit_nit@yahoo.co.in

SUMMARY

This research aims to determine the static response of an arch dam before undertaking a dynamic analysis of the dam due to hydrodynamic and seismic stresses. An arch dam with soil interaction, a dam without soil contact, and a dam between soil and reservoir system were all modelled using ANSYS finite element software. The research intends to determine various deformations and stresses caused by the loads attributed to arch dams in different dam systems. Many different outcomes are mapped out and discussed, mainly as weight differences.

KEY WORDS: concrete arch dam; Finite element method; ANSYS FEM models; static analysis.

1. INTRODUCTION

Concrete arch gravity dams are aesthetically pleasing due to their arch construction between two hills, which creates new design challenges for their application roles in irrigation, cultivation, flood safety, and generating renewable energy implemented for a nation's development and sustainability. The form arch dam has a structural feature that permits hydrostatic pressure to be redirected along the dam. They are geometrically complicated structural systems with varied irregular centers of external and interior arches and different exterior and interior radius or arc angles. The stability behavior of these dams owing to static pressures may impact their durability, safety, and life comfort, resulting in social, financial, and ecological losses. So this study aims to resolve an arch dam's static response, which must be determined before a dynamic analysis of the dam.

Rizwan Ali et al. [1] performed a simulated stress study on a concrete gravity dam to determine its structural integrity under dynamic loads during an earthquake. When performing such analysis with general-purpose FEM software, a pseudo-static technique with constant seismic coefficients is often applied. This method, however, may be too cautious, resulting in extraordinarily high stresses in the dam body. The findings of a finite element-based two-dimensional 2D static and pseudo-dynamic stress analysis were reported. The estimated stresses for different load combinations were compared to the allowed stresses and specified strength of concrete. Zhuan-Yun [2] investigated the exact bearing properties and seismic

dynamic characteristics of the large scale hydro-power station's high arch dam and established a 3D finite element numerical model of the interface configured between both the arch dam and foundation, based on the ANSYS to perform static analysis under basic combined effects, and dynamic behaviour under important factors affecting the elevated arch dam. Swapnal and Awari [3] used ANSYS finite element analysis software to investigate the influence of soil interaction on gravity dams. The investigation revealed that, when soil stiffness and the bulk of the soil are considered, displacement is better for dams with soil foundation interfaces than for dams without soil foundation interfaces. Ajayakumar et al. [4] aimed to create an FEA model of a concrete arch gravity dam that could be used to investigate stress and deformation in an arch dam. The model analysis findings did not show any regions of stress. As a result, it may be asserted that the specified stresses are likely to be within the recognised threshold under available loading conditions. Gupta and Minoti Das [5] contend that simplified techniques for gravity dam construction that mimic dynamic loads by equivalent static loads cannot anticipate correct physical behaviour. A comprehensive dynamic response study must be performed to provide a realistic approximation of the structural reaction under dynamic loads. A comprehensive dynamic response analysis of the dam's seismic safety is needed. An extensive dynamic response study of the dam's highest non-overflow and overflow parts was undertaken using site-specific design and trustworthy accelerograms to assess the dam's stability. The reservoir is modelled using the fluid acoustic element FLUID 29, and the dam and foundation are modelled using the 2D planar strain element PLANE 42 with an adequate account of fluid-structure interaction. Based on modal analysis, a formulation for the basic period of concrete dams is established. Varughese and Nikithan [6] used the finite element application ANSYS to evaluate static, modal, and transient studies of the dam reservoir-foundation system. The reservoir is modelled using the fluid acoustic element FLUID 29 and the dam and foundation are modelled using the 2D planar strain element PLANE 42 with an adequate account of fluid-structure interaction. Based on modal analysis, a formulation for the basic period of concrete dams is established. Soumya et al. [7] used ANSYS to compare a 3D model of a monolith gravity dam to the analogous 2D model. They found that a modal analysis of 3D models revealed the existence of out-of-plane frequency that 2D models did not. Consequently, for load evaluations, the 3D models show higher stress increase than the 2D ones. Higher tensile stresses are created for 3D models at the heel of a shorter cross-section for hydrostatic loads. Margaret Abraham et al. [8] created a computer simulation of gravity dam structural reaction that considered the foundation-structure interaction. The ideal numerical model foundation depth and width were also examined. Foundation stiffness-based parametric analysis was performed. The Peechi gravity dam case study illustrates the principle. Dam structural study should incorporate foundation-structure interaction, according to the research. Foundation-structure and fluid-structure interactions might enhance the gravity dam seismic analysis computer model.

The primary goal of this study is to use ANSYS software to perform stability analysis for 3D finite element concrete arch gravity dam models with diverse configurations owing to various combinations of static forces.

2. MODELLING OF A DAM

2.1 DAM DIMENSIONAL CONFIGURATIONS AND MATHEMATICAL IDEALIZATION OF A DAM

The dam's geometry variables are presented in Table 1, while Figure 1 depicts a cross-section of the dam with geometry variables. This article investigates the planned concrete arch gravity dam project at Jankar Jangal near Chamba in Himachal Pradesh's Ravi River basin.

Table 1 The geometry variables of the dam

Concrete dam	Model Type	Arch dam (m)	
	Crest width	4	
	Base width	36.3	
	Height	25.94	
	Length	20.05	
	Maximum depth in water	25.44	
Foundation soil	Model Type	Soil layer 1 (supporting Dam) in m	Soil layer 2 (below the dam) in m
	X coordinates	27	30
	Y coordinates	48.3	72
	Z coordinates	95	115

The finite element method (FEM) has evolved into a powerful tool for solving numerically various engineering challenges. In this work, the concrete arch gravity dam was modelled using the finite element-based software ANSYS [9-11]. The three different types of discretization of the model dam are shown in Figures 2-4, respectively. To investigate the stability behaviour of the dam due to various combinations of static loads, three different model cases are dealt with, as follows.

- Model 1: Dam with fixed support (dam devoid of soil foundation) and an empty reservoir named "fixed-empty" (Figure 1).
- Model 2: "mass-empty" dam with soil foundation and empty reservoir (Figure 2).
- Model 3: "mass-fluid" dam with soil foundation and full reservoir (Figure 3).

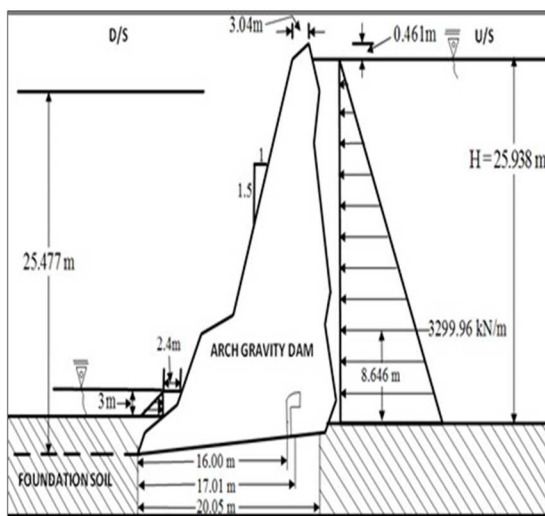


Fig. 1 The Geometry of the concrete arch gravity dam

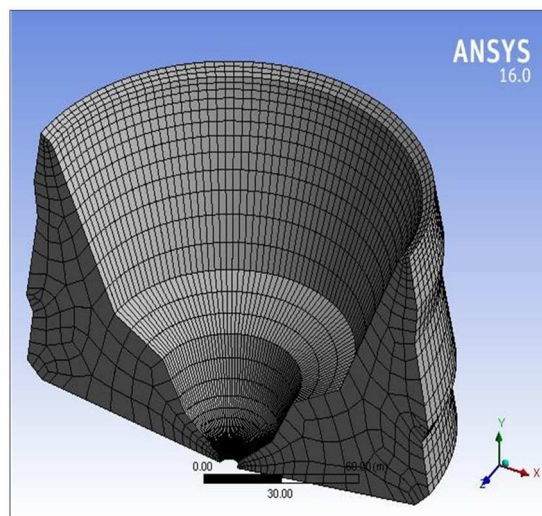


Fig. 2 Model 1 Dam without soil foundation model

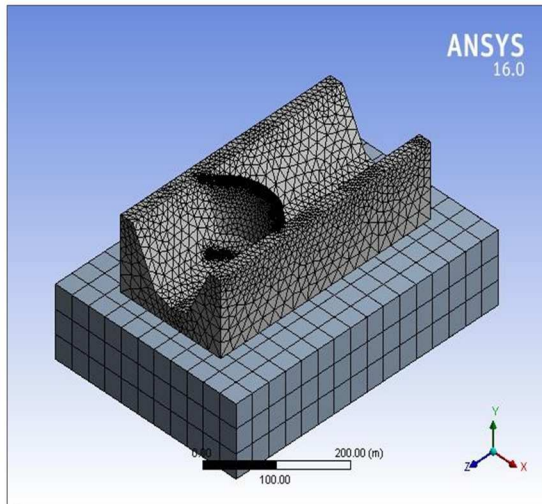


Fig. 3 Model 2 Dam with soil foundation model

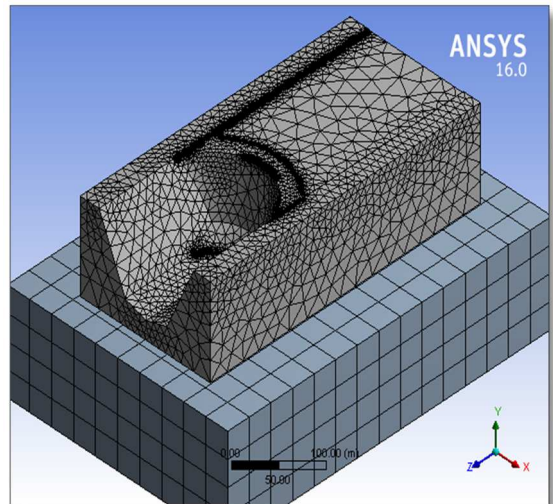


Fig. 4 Model 3 Dam with soil and reservoir

The dam is assumed to be a fixed boundary constraint at the base of model 1 and fixed at the base of the foundation for models 2 and 3. The length of the reservoir is defined as 1.5 times the depth. Each element's node has six degrees of freedom, which include translations and rotations in the X, Y, and Z dimensions.

2.2 MATERIAL PROPERTIES

Table 2 shows the material characteristics of concrete arch dams and foundation soils, as well as of the reservoir water. Various organizations need this information for safe construction. The mass of concrete is considered homogenous, isotropic, and elastic. The ideal foundation soil is a homogeneous, isotropic, and elastic medium.

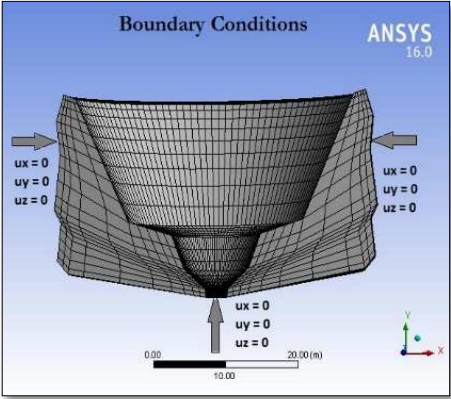
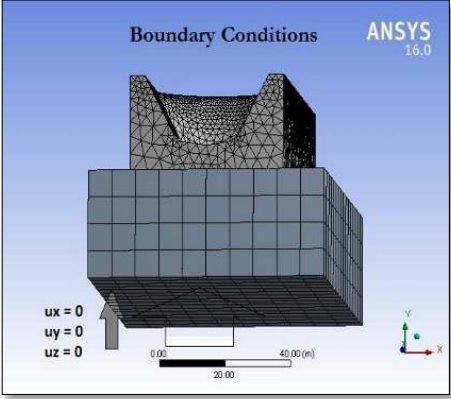
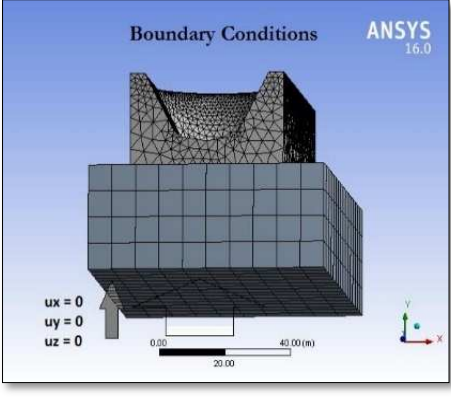
Table 2 Material properties of the concrete dam, reservoir water, and foundation soil

Concrete dam	Mass density of concrete (ρ) kg/m ³	2500
	Modulus of elasticity of concrete (E) MPa	28500
	Poisson's ratio (μ)	0.2
Reservoir water	Density of water (ρ) kg/m ³	1000
	Bulk modulus of elasticity of water (K) MPa	2020
	Sonic velocity or Speed of pressure wave (m/s)	14500
Foundation soil	Wave reflection coefficient	0.25
	Mass density of foundation Soil (ρ) kg/m ³	2100
	Modulus of elasticity of foundation soil (E) MPa	14500
	Poisson's ratio (μ)	0.25

2.3 ANALYSIS ELEMENT TYPES AND BOUNDARY CONDITION

The element types and boundary conditions used for dam analysis are listed in Table 3.

Table 3 Element types and boundary condition

<i>(I) Element Types</i>	
<i>Model</i>	<i>Element types</i>
<i>Concrete dam</i>	<i>3D solid element</i>
<i>Reservoir water</i>	<i>3D solid element</i>
<i>Foundation soil</i>	<i>3D solid element</i>
<i>(II) Boundary Condition</i>	
<i>Model</i>	<i>Boundary Condition</i>
<i>Model 1: Dam devoid of soil foundation and an empty reservoir, named "fixed-empty" (Figure 1).</i>	<p>The dam is assumed to be a fixed boundary constraint at the base</p> 
<i>Model 2: Dam with soil foundation and empty reservoir, named "mass-empty" (Figure 2).</i>	<p>Fixed at the base of the foundation for the model 2</p> 
<i>Model 3: Dam with soil foundation and full reservoir, named "mass-fluid" (Figure 3).</i>	<p>Fixed at the base of the foundation for the model 3</p> 

2.4 FORCES CONSIDERED IN THE STABILITY ANALYSIS OF ARCH DAMS

The forces that an arch gravity dam must withstand are divided into two groups:

- a) forces that can be evaluated directly from material unit weights and fluid pressure properties, such as dam weight and water pressure;
- b) factors that can only be assumed with varied degrees of certainty like uplift, seismic forces, silt pressure, ice pressure, wave pressure, wind pressure, and thermal loads.

The forces acting on a dam are not all exerted at the same time. Several load combinations may operate concurrently. The dam's design is based on the most unfavourable combination of possible load circumstances. Based on IS 6512:1984, the following adverse load combinations are considered in the present analysis of the dam.

- Load combination A (Construction): The dam is completed but the reservoir and tailwater are empty.
- Load combination B: Reservoir is full, tailwater with usual rise, ice, and silt under dry conditions (if present).
- Load combination C: All gates are open, the reservoir is at maximum flood water height, the tailwater is at flood level, the uplift is normal, and silt is present (if applicable).
- Load combination D: A and an earthquake.
- Load combination E: B with an earthquake but no ice.
- Load combination F: C with a lot more uplift (drains inoperative).
- Load combination G: E with a lot more uplift (drains inoperative).

2.5 DAM STABILITY REQUIREMENT

The following are the fundamental stability criteria for a gravity dam, as defined by the IS: 6512-1984 code, under all loading circumstances when treating the dam-foundation system as a monolith, and the design must meet the following stability requirements:

- (i) The dam shall be safe against overturning in any horizontal plane within the structure, including at and below the base.
- (ii) Sliding on any plane or combination of planes inside the dam and at and within the foundation must be safe.

3. RESULTS AND DISCUSSION

The foundation and water reservoir obviously influence the static response and, as a result, the dynamic response of gravity dams during earthquakes. Stability analysis of the various FEM dam model models is performed, and a comparative study on the deformation and stress is depicted in Figures 17-23.

3.1 FORCES CALCULATIONS

The different forces acting on the U/S and D/S sides of the arch dam are estimated, as shown in Figures 5-7, and obtained values are used as inputs in ANSYS workbench software. The results

are then compared, and failure is considered. Important results from the finite element analysis are depicted as contours across the dam section for static load combinations A and B in Figures 5-14, and for static earthquake load combinations D, E, and G in Figures 17-21. These figures compare the maximum values of stresses and displacements for different loads and load combinations. The values of stresses and displacements increased significantly due to earthquake loads.

3.2 STABILITY ANALYSIS NEGLECTING SEISMIC FORCES

3.2.1 RESERVOIR EMPTY CONDITION

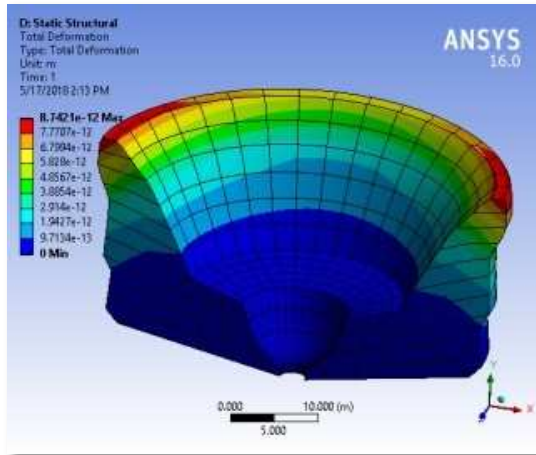
Load combination A: The dam is built but there is no water in the reservoir and no water coming out of the dam.

Table 4 Gravitational vertical load calculation

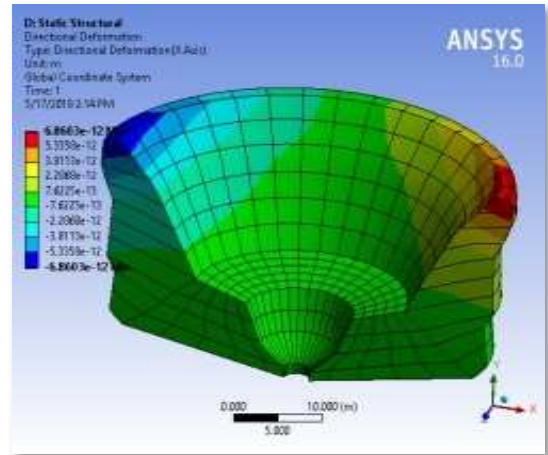
Item	Forces in kN		Lever Arm in m (from the heel)	Moment at toe in kN-m	
	V	H		(m _v)	(m _H)
<i>(I) Gravitational vertical weight</i>					
<i>(a) Self weight of concrete arch gravity dam (w) Reservoir empty condition</i>					
$(w_1) = L * B * D * \gamma$ $= 1 * 3.04 * 25.938 * 23.5$	1853.0	-	$17.01 + \frac{3.04}{2} =$ $= 18.53$	34336.09	-
$(w_2) = \frac{1}{2} * L * B * D * \gamma$ $= \frac{1}{2} * 1 * 17.01 * 25.477 * 23.5$	5092.0	-	$\frac{2}{3} * 17.01 =$ $= 11.34$	57743.28	
<i>Sum of Table 3</i>	$\sum V_1 = 6945$			$\sum M_1 = 92079.37$	

Figure 5-7 depicts how the weight of concrete arch gravity bends and stresses dams without a soil basis, dams with a soil base, and dams with a soil foundation plus a reservoir. Figures 5 and 6 show that the dam with soil and reservoir reduce total deformation, directional deformation (x, y, z axis), normal stress, and equivalent (Von-Misses) stress for self-weight (dead load).

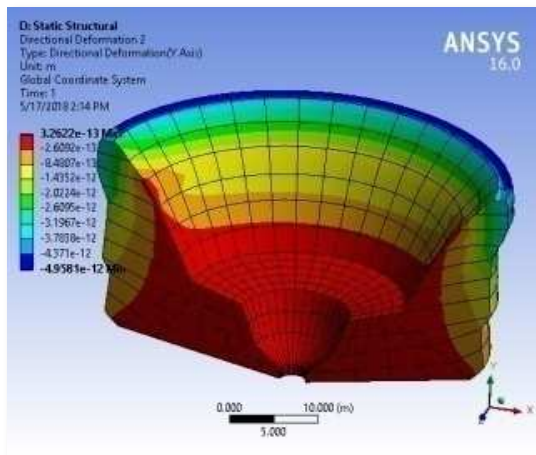
(a) Total deformation of the dam



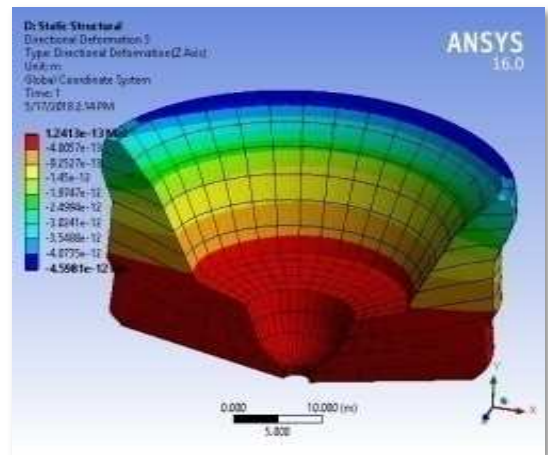
(b) Directional deformation (X-axis)



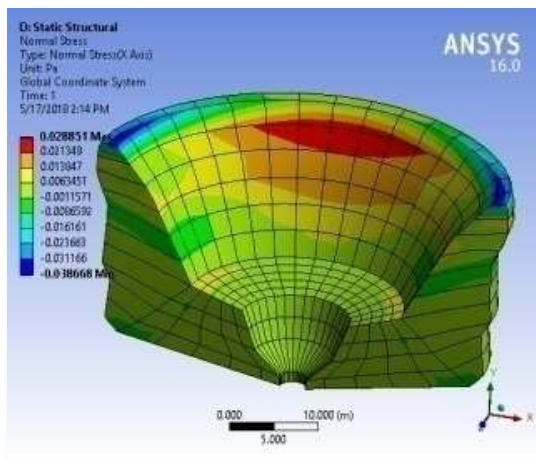
(c) Directional deformation (Y-axis)



(d) Directional deformation (Z-axis)



(e) Normal stress acting on the dam



(f) Equivalent (Von-Mises) stress

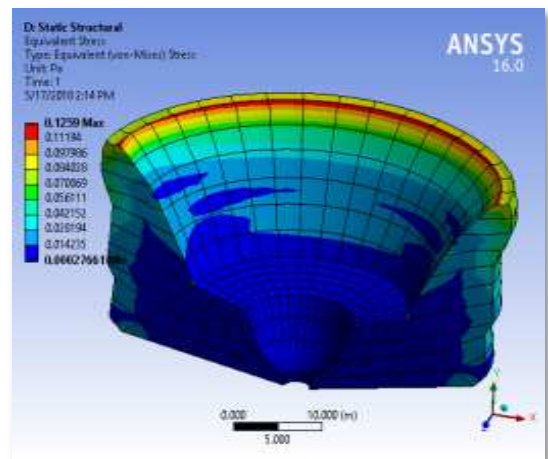


Fig. 5 Self-weight-induced deformation and stresses on a dam (without a soil foundation)

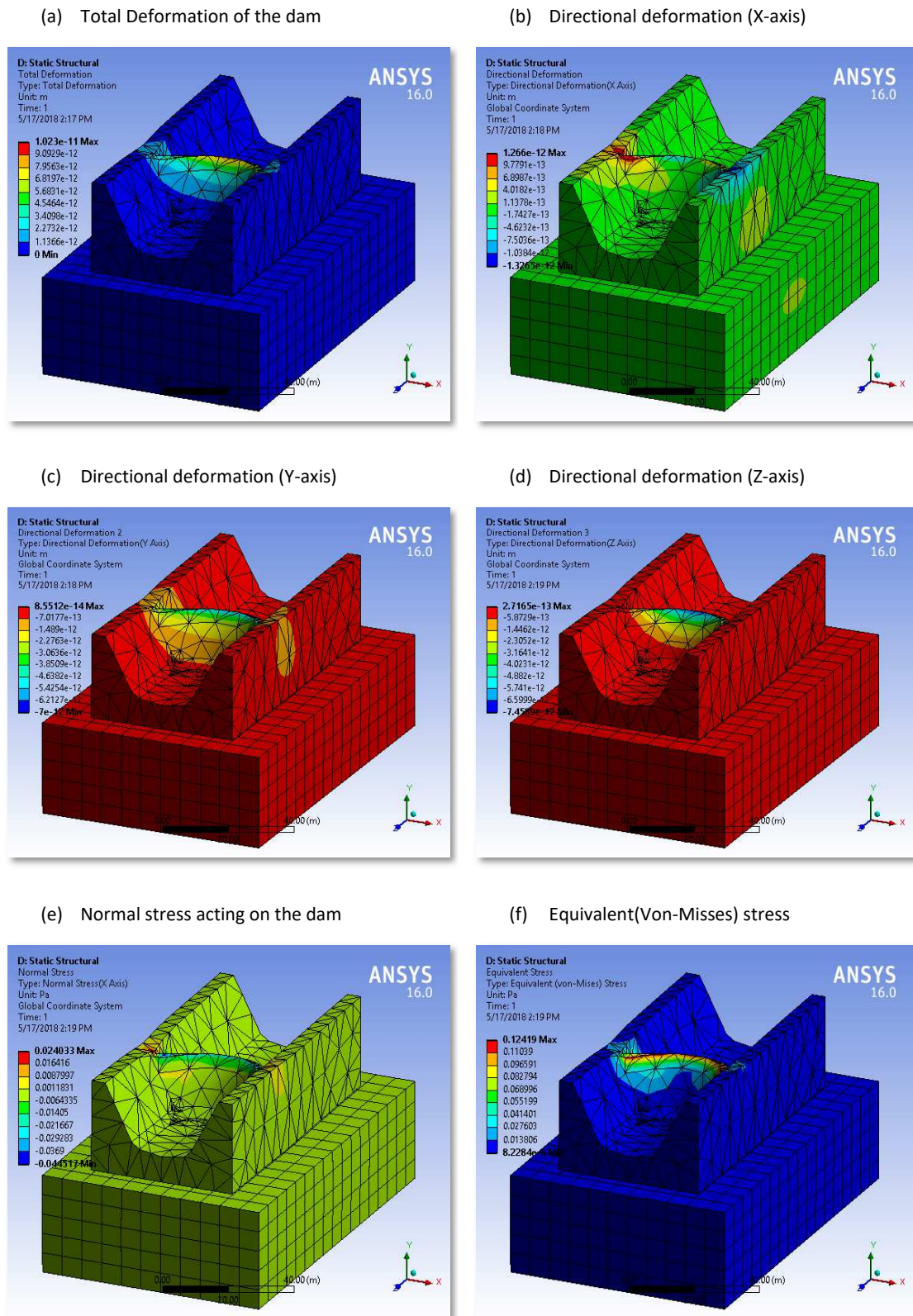
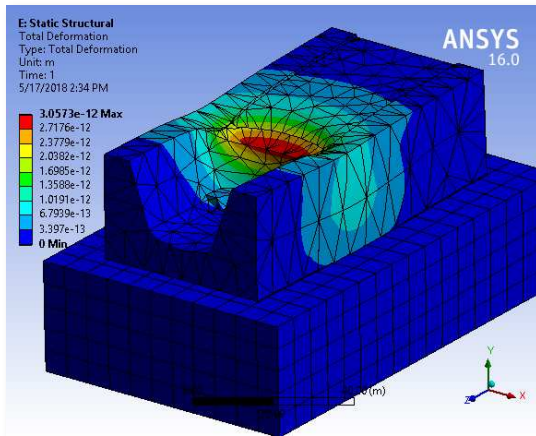
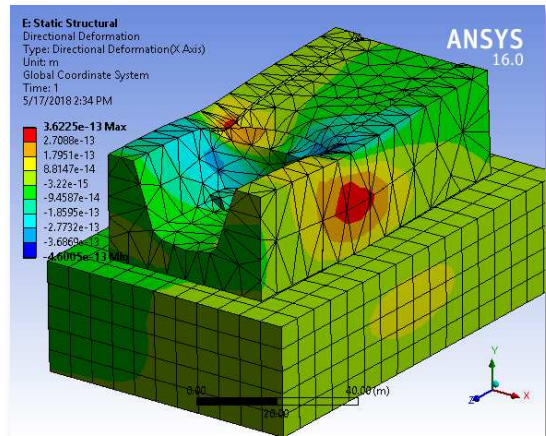


Fig. 6 Self-weight-induced deformation and stresses on a dam (with a soil foundation)

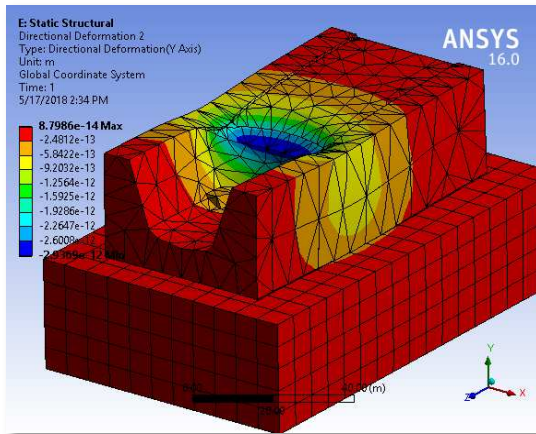
(a) Total deformation of the dam



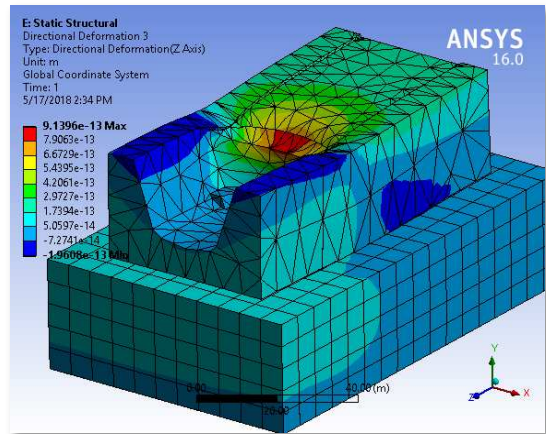
(b) Directional deformation (X-axis)



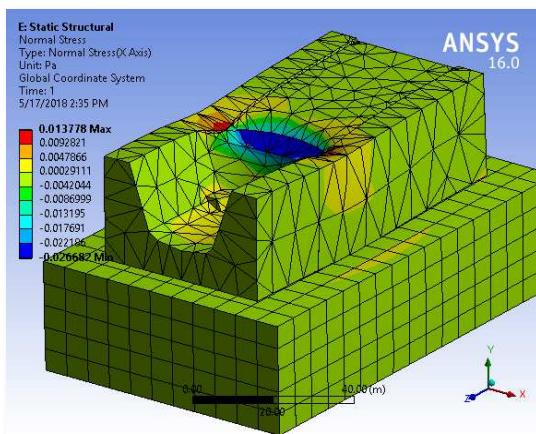
(c) Directional deformation (Y-axis)



(d) Directional deformation (Z-axis)



(e) Normal stress acting on the dam



(f) Equivalent (Von-Mises) stress

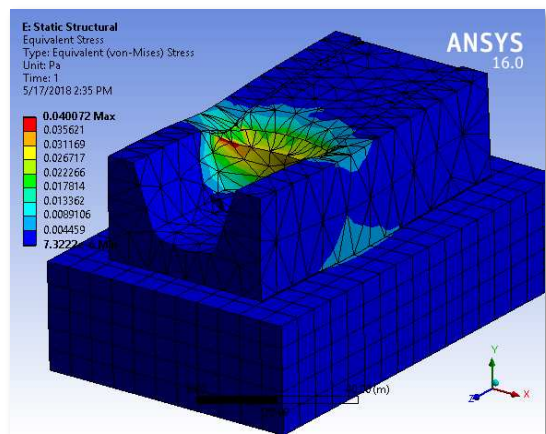


Fig. 7 Deformation and stresses due to self-weight acting on a dam (soil foundation, reservoir)

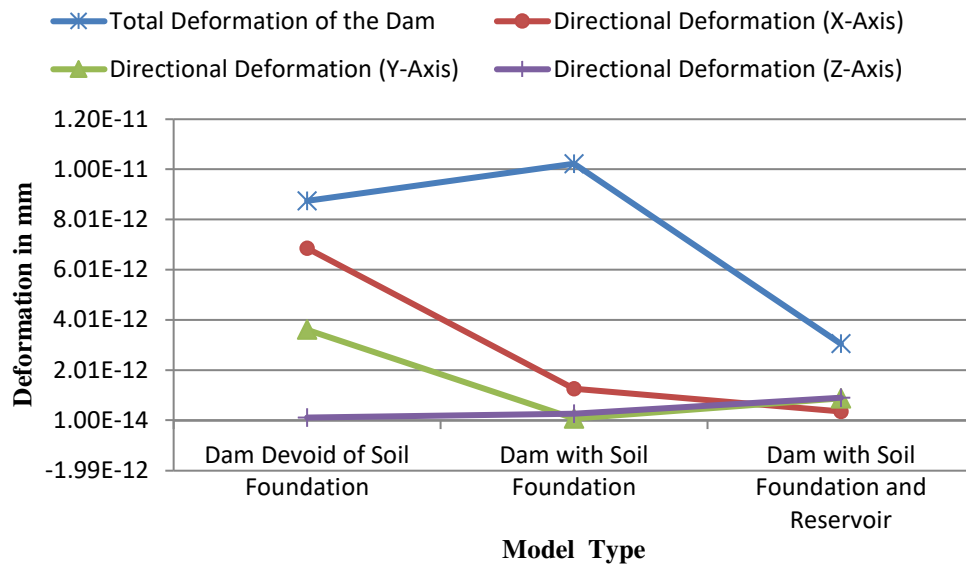


Fig. 8 Various deformations of various dam models due to their self-weight

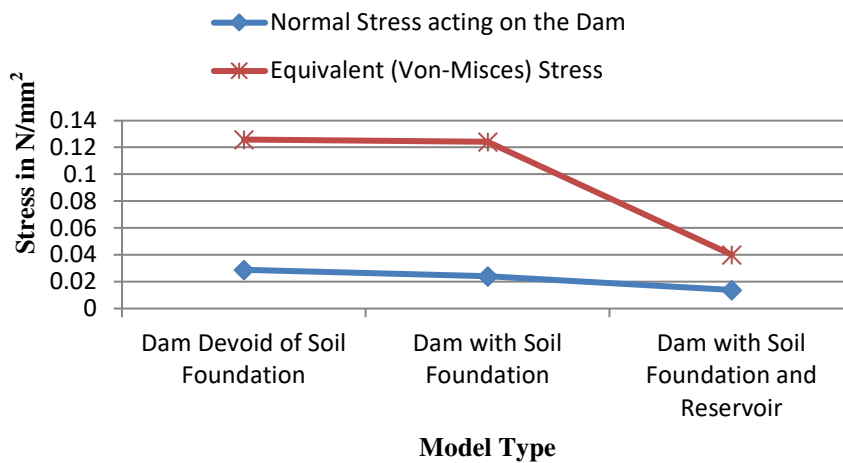


Fig. 9 Various stresses of various dam models due to the self-weight of the dam

3.3 THE RESERVOIR IS FULL WITH NO UPLIFT

Load combination B: The reservoir is at full capacity and tailwater in normal dry conditions, normal rise, ice, and silt (if present) (Figure 10).

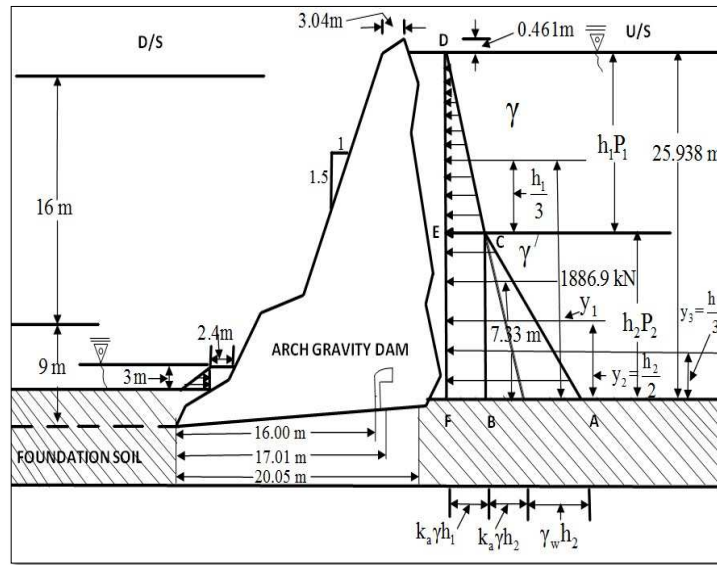
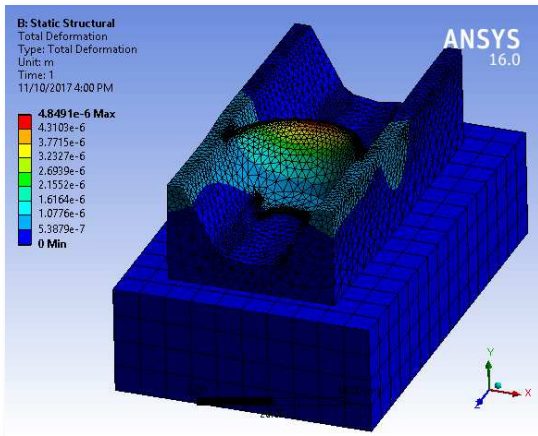


Fig. 10 Concrete arch gravity dam geometry with water lateral pressure

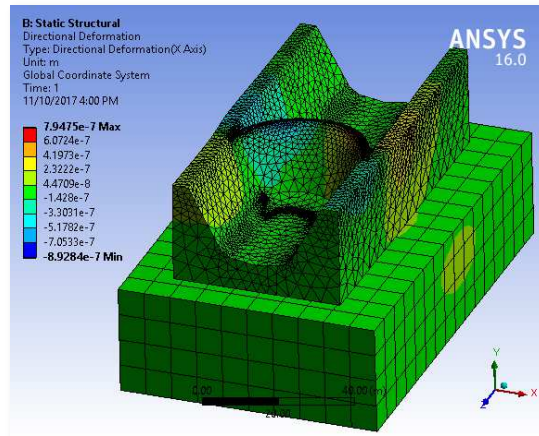
Table 5 Calculation of gravitational vertical load, horizontal water pressure, and vertical gravity weight of water

(II) Weight of water					
Item	Forces in kN		Lever Arm in m (from the Heel)	Moment at toe in kN-m	
	V	H		(mv)	m(H)
(b) Weight of water on D/S [Reservoir full condition]					
$(w') = \frac{1}{2} * \gamma * H * B = \frac{1}{2} * 9.81 * 3 * 2.4$	35.316	-	$\frac{1}{3} * 2.4 = 0.8$	28.252	
(III) Horizontal water pressure and vertical gravity weight of water [reservoir full with no uplift pressure]					
(a) Water Pressure on U/S of Gravity Dam with Concrete Arch					
$(P) = \frac{1}{2} * \gamma * H * H = \frac{1}{2} * 9.81 * 25.938 * 25.938$		3299.985	$\frac{1}{3} * 25.938 = 8.646$		28531.67
(b) Water Pressure on D/S of concrete Arch Gravity Dam					
$(P') = \frac{1}{2} * \gamma * H * H = \frac{1}{2} * 9.81 * 3 * 3$		44.145	$\frac{1}{3} * 3 = 1$		44.145
(c) Weight of super Imposed column of Water on D/S					
$(\hat{w}_1) = \frac{1}{2} * \gamma * H * B = \frac{1}{2} * 9.81 * 3 * 2.4$	35.316		$16 + \frac{2}{3} * 3 = 18$		635.688
$(\hat{w}_2) = \gamma * H * B = 9.81 * 22.94 * 8$	1800.33		$16 + \frac{1}{2} * 3 = 17.5$		31505.796
$(P_w) = \frac{1}{2} * \gamma * H * H = \frac{1}{2} * 9.81 * 25.938 * 25.938$		3299.985	$\frac{1}{3} * 25.938 = 8.646$		28531.67
Sum of Table 3+ Table 7	$\sum V_2 = 8815.962$				$\sum M_2 = 92079.37$

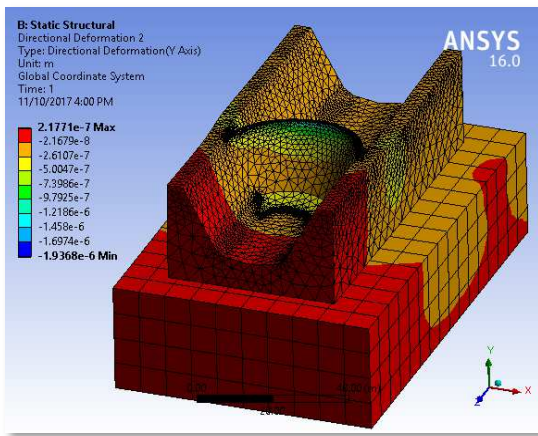
(a) Total deformation of the dam



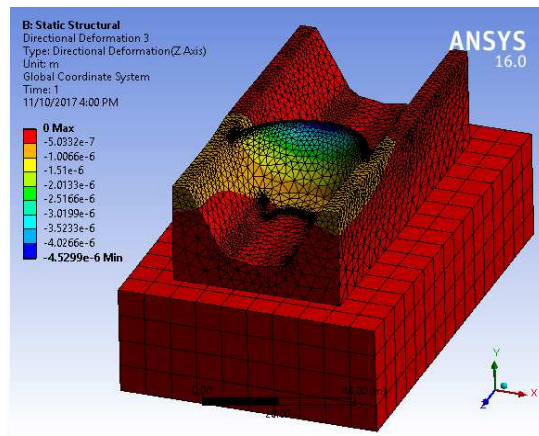
(b) Directional deformation (X-Axis)



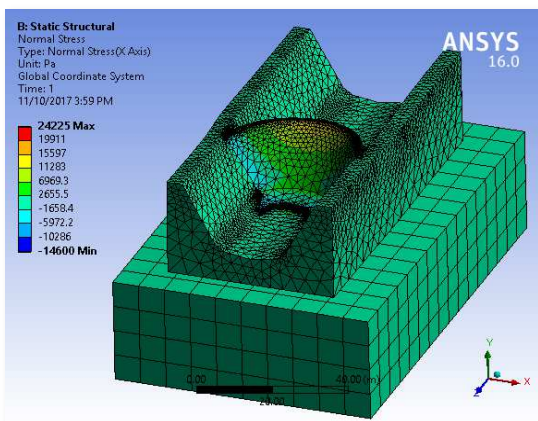
(c) Directional deformation (Y-Axis)



(d) Directional deformation (Z-Axis)



(e) Normal stress acting on the dam



(f) Equivalent (Von-Mises) stress

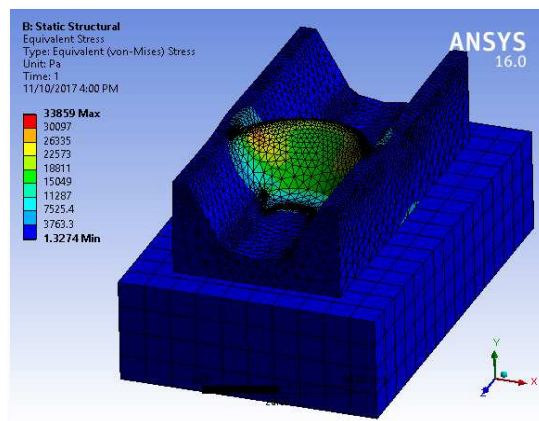


Fig. 11 Results of simulating the effects of water pressures on the upstream and downstream sides of the arch dam

3.4 RESERVOIR FULL WITH UPLIFT CONDITION

Load combination B: The reservoir is at full capacity, tailwater in normal dry conditions, normal rise, ice, and silt (if present) (Figure 12).

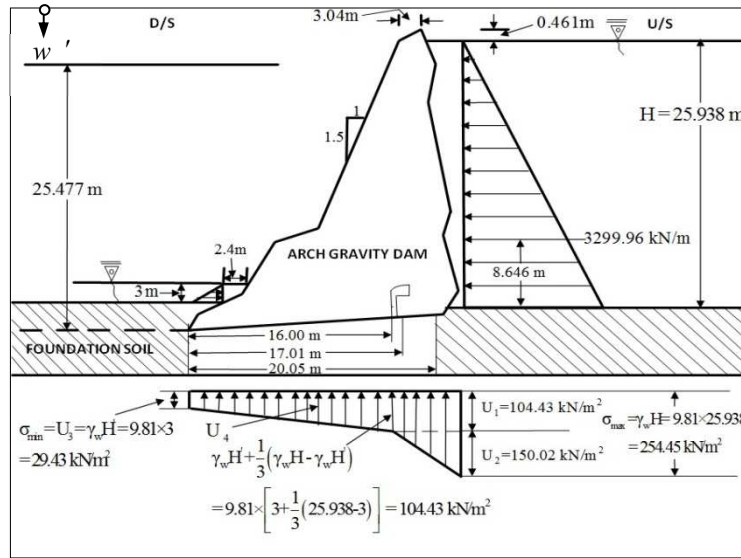
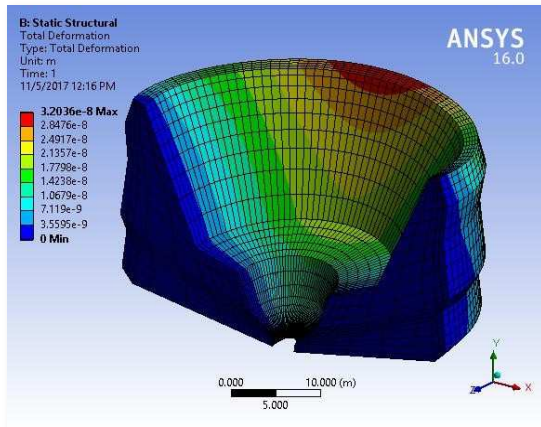


Fig. 12 The geometry of a concrete arch gravity dam with water pressure from above and from the sides

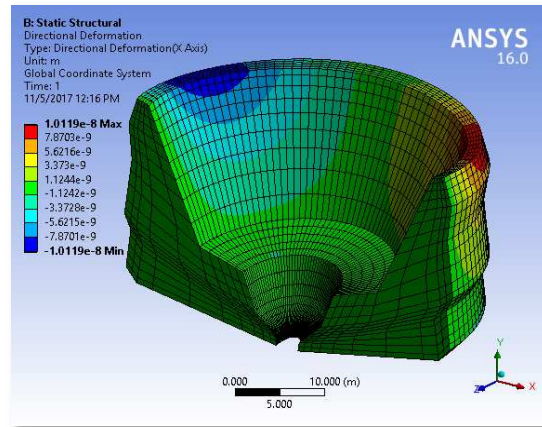
Table 6 Calculation of the uplift water pressure at the dam's base

(III) Uplift Water Pressure (Pu) [Reservoir Full Condition]					
Item	Forces in kN		Lever Arm in m (from the Heel)	Moment at toe in kN-m	
	V	H		(m _V)	(m _H)
$(U_1) = \sigma_{max_{u_1}} * B * L = 104.43 * 4 * 1$	-417.72		$16 + \frac{4}{2} = 18$		7518.96
$(U_2) = \frac{1}{2} \sigma_{max_{u_2}} * B * L = \frac{1}{2} * 150.02 * 4 * 1$	-300.04		$16 + \frac{2}{3} * 4 = 18.66$		5600.74
$(U_3) = \sigma_{min_{u_3}} * B * L = 29.43 * 16 * 1$	-470.88		$\frac{16}{2} = 8$		3767.04
$(U_4) = \frac{1}{2} \sigma_{max_{u_4}} * B * L = \frac{1}{2} * 75 * 16 * 1$	-600		$\frac{2}{3} * 16 = 10.66$		6400
Sum of Table 4+ Table 7 + Table 9	$\sum V_2 = 8815.962$				$\sum M_2 = 92079.37$

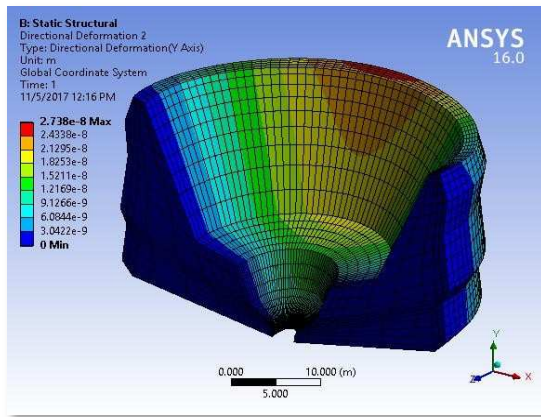
(a) Total Deformation of the dam



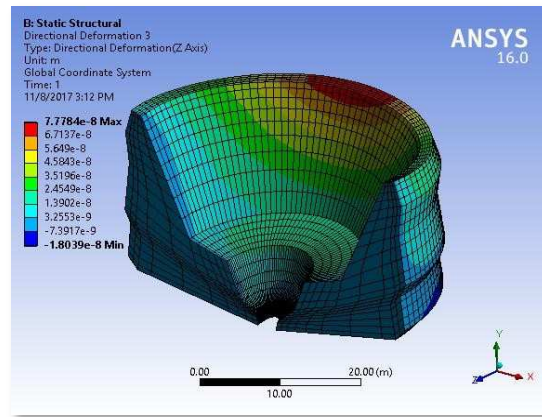
(b) Directional Deformation (X-Axis)



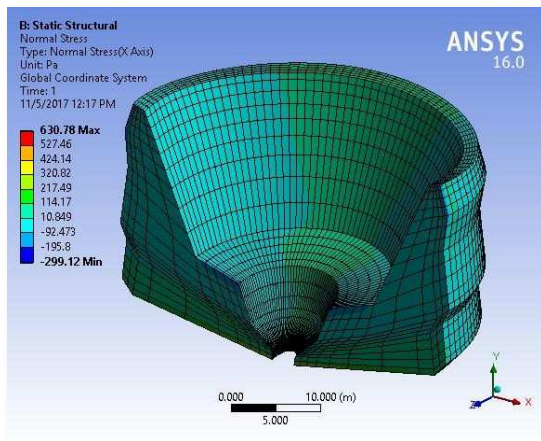
(c) Directional Deformation (Y-Axis)



(d) Directional Deformation (Z-Axis)



(e) Normal Stress acting on the Dam



(f) Equivalent (Von-Mises) Stress

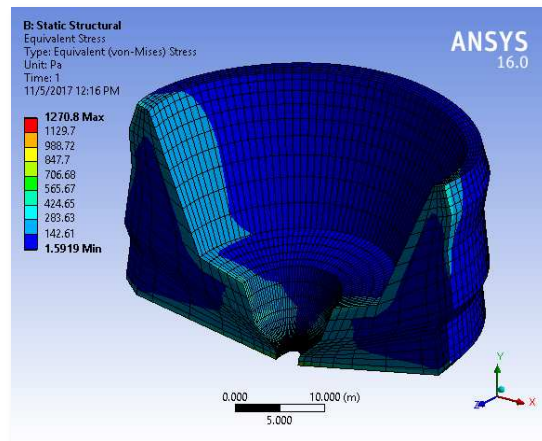


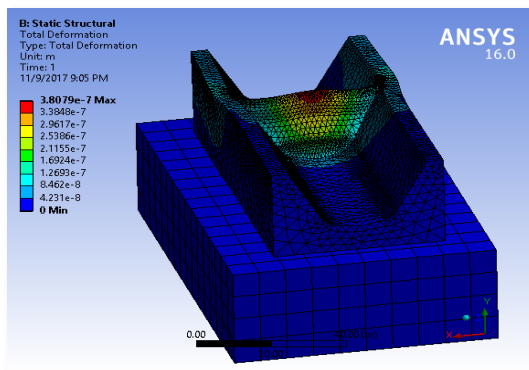
Fig. 13 Results of simulated uplift water pressure acting at the dam's bottom face

3.5 THE UPSTREAM FACE OF THE CURVATURE DAM CONDITION HAD SILT PRESSURE APPLIED TO IT

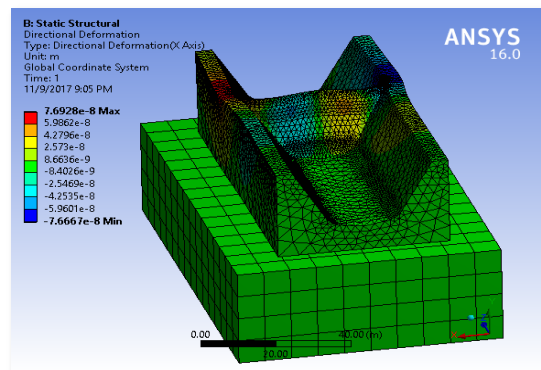
Table 7 Calculation of the silt pressures exerted on a dam's upstream side

<i>(III) Silt Pressure (P_s) [Reservoir Full Condition]</i>					
Item	Forces in kN		Lever Arm in m (from the Heel)	Moment at toe in kN-m	
	V	H		(m_V)	(m_H)
$(P_{s_1}) = \frac{1}{2} * K_a * \gamma_{top\ moist\ slit} * h_1 * h_1$ $= \frac{1}{2} * 0.271 * 18 * 16 * 16$		624.384	$\left(h_2 = 9 + \frac{h_1 = 16}{3} \right) =$ $= 14.33$		
$(P_{s_2}) = K_a * \gamma_{top\ moist\ slit} * h_1 * h_2$ $= 0.271 * 18.8 * 16 * 9$		733.651	$\left(\frac{h_2 = 9}{2} \right) = 4.5$		
$(P_{s_3}) = \frac{1}{2} * \gamma_w * h_2 * h_2 + \frac{1}{2} * K_a * [\gamma_{submerge\ slit} = \gamma_{sat} - \gamma_w] * h_2$ $= \frac{1}{2} * 9.81 * 9 * 9 + \frac{1}{2} * 0.271 * [21.8 - 9.81] * 9 * 9$		528.901	$\left(\frac{h_2 = 9}{3} \right) = 3$		
$\sum P_s = 1886.936\text{ kN}$					
Resulting Horizontal Thrust / m length of the dam wall acting 1886.936 kN at 7.3323 from the base					

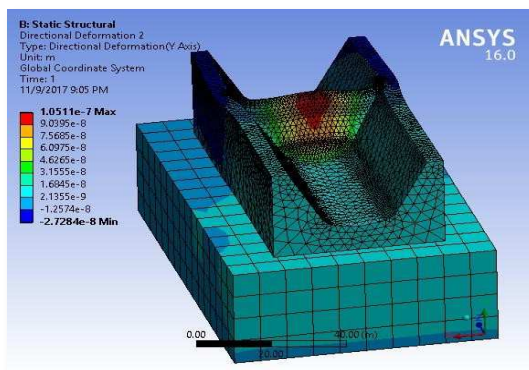
(a) Total Deformation of the dam



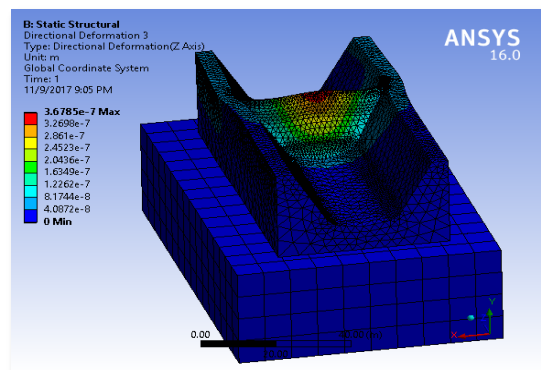
(b) Directional Deformation (X-Axis)



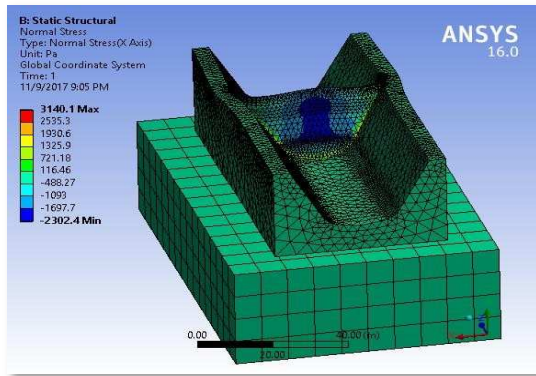
(c) Directional Deformation (Y-Axis)



(d) Directional Deformation (Z-Axis)



(e) Normal Stress acting on the Dam



(f) Equivalent (Von-Mises) Stress

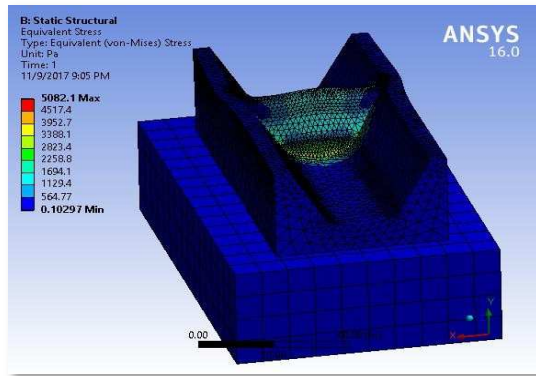


Fig. 14 Simulated effects of silt pressures on the dam's upstream side

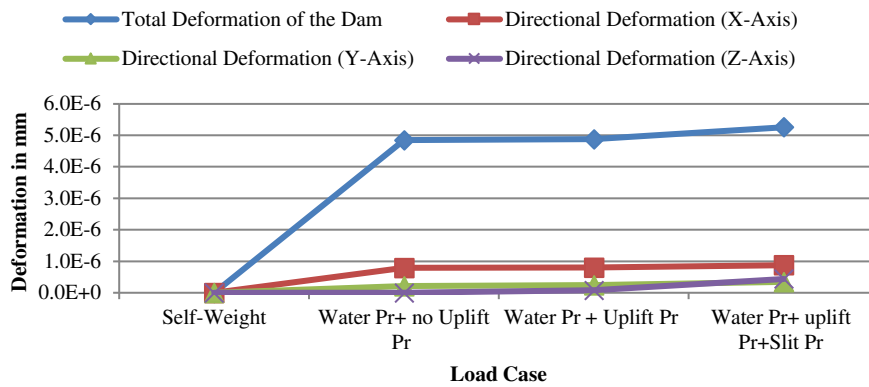


Fig. 15 Various deformations of the dam with soil foundation model due to various load cases

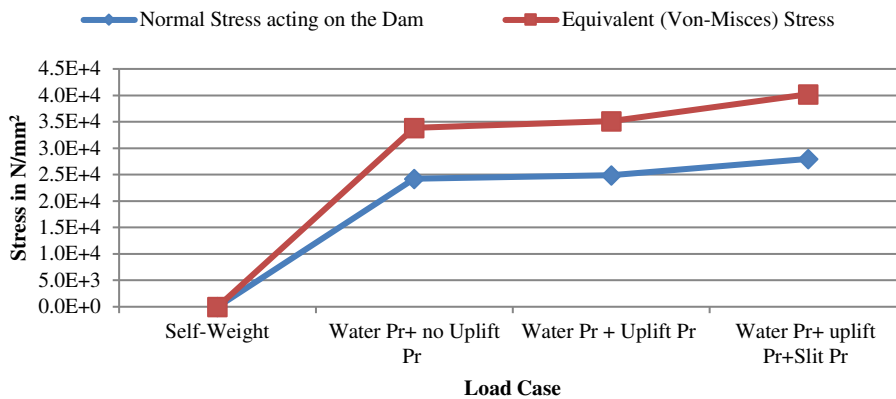


Fig. 16 Various stress of dam with soil foundation model due to various load case

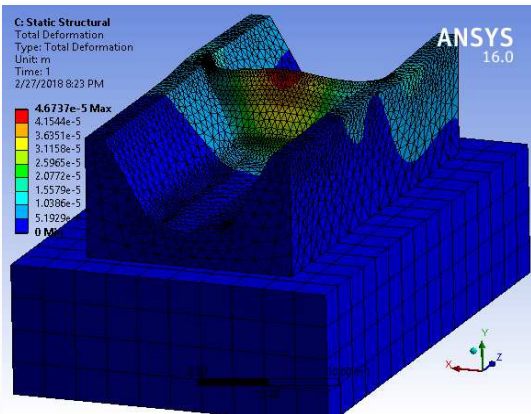
Figure 15 and Figure 16 show that horizontal water pressure on dam acting on U/S and D/S face, uplift pressure, and slit pressure increase the total deformation, directional deformation (x, y, z axis), normal stress, and equivalent (Von-Mises) stress.

3.6 STABILITY ANALYSIS CONSIDERING SEISMIC FORCES

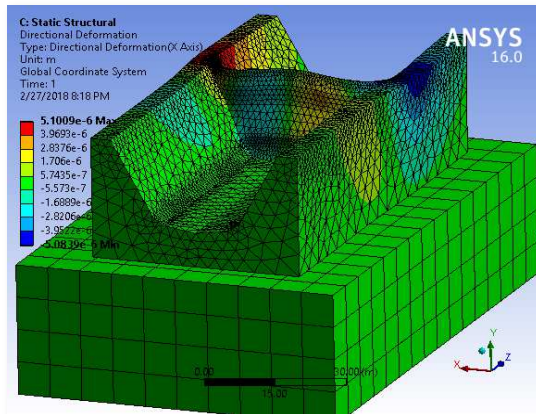
Table 8 Calculation of the forces operating on an arch dam from hydrodynamics, horizontal inertia, and vertical acceleration

Item	Forces in kN		Lever Arm in m (from the Heel)	Moment at toe in kN-m
	V	H		
Horizontal Earthquake Pressure $P_{w_1} = -0.1 * (w_1) = -0.1 * 1853.0$ $P_{w_2} = -0.1 * (w_2) = -0.1 * 5092.0$		185.3	$\left(\frac{h_2=9}{3}\right) = 3$	-555.9
		509.2	$\left(\frac{25}{3}\right) = 8.33$	-4241.63
$\sum H_1 = -692.5$		$\sum M_1 = -4797.53$		
Vertical Earthquake Pressure $\sum V_2 = -0.005 \sum V_1 = -0.005 * 6945$	34.725			$\sum M_2 = 0.05 \sum M_1$ $= 0.05 * 92079.37$ $= 4603.968$
Upward Vertical Earthquake Pressure $\sum V_2 = -0.05 \sum V_1 = -0.05 * 6945$	347.25			$\sum M_2 = 0.05 \sum M_1$ $= 0.05 * 92079.37$ $= 4603.968$
Horizontal Hydrostatic Pressure $(P) = -\frac{1}{2} * H * H = -\frac{1}{2} * 25.938 * 25.938$	-336.389		$\frac{1}{3} * 25.938 = 8.646$	-2908.419
$(P') = \frac{1}{2} * H * H = \frac{1}{2} * 3 * 3$	4.5		$\frac{1}{3} * 3 = 1$	4.5
	$\sum H_1 = -331.889$			$\sum M_4 = -2903.919$
Horizontal Hydrodynamic Pressure $\sum H_2 = (P_e) = -0.729 * p_e = \left[C_m = 0.69 \frac{\left(\theta = \tan^{-1} \left(\frac{H}{2} \right) \right)}{90^\theta} \right] K_h \gamma_w H * H$ $= -0.729 * \left[C_m = 0.69 \frac{\left(\theta = \tan^{-1} \left(\frac{25.938}{2} = 12.969 \right) = 85.59^\theta \right)}{90^\theta} \right] = 0.69 * 0.1 * 9.81 * 25.938 = 17.89 * 25.938$ $= -356.839$				$(M_e) = 0.412 * (P_e) * H$ $= 0.412 * -356.839 * 25.938$ $= 3813.351$
Horizontal inertia force due to earthquake $-0.1w_1 = -0.1 * 1853.0$ $-0.1w_2 = -0.1 * 5092.0$	-185.3		$\frac{9}{3} = 3$	-555.9
	-509.20		$\frac{25}{3} = 8.33$	-4241.636
	$\sum H_3 = -694.5$			$\sum M_7 = -4797.536$
$\sum H_1 = \sum H_1 + \sum H_2 + \sum H_3$	$= -331.889 - 356.839 - 694.5 =$ $= -1383.228$			

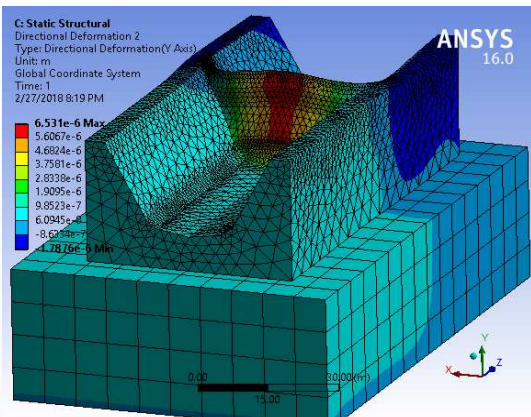
(a) Total Deformation of the dam



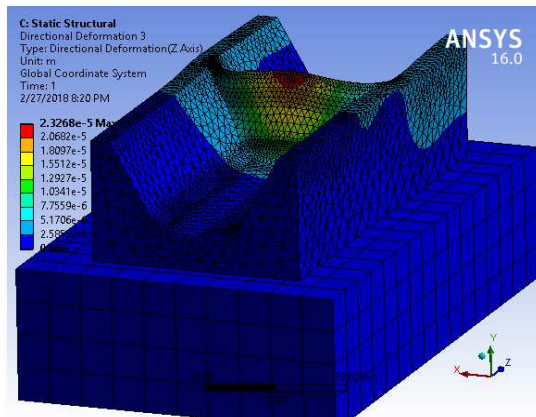
(b) Directional Deformation (X-Axis)



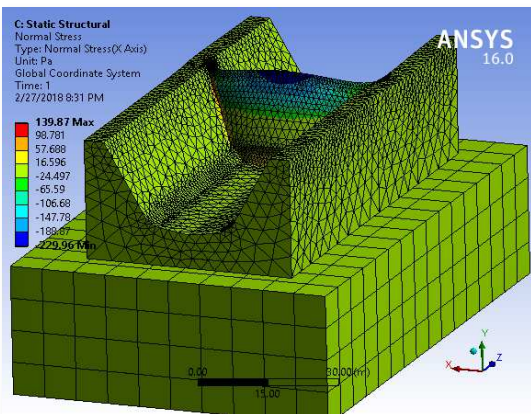
(c) Directional Deformation (Y-Axis)



(d) Directional Deformation (Z-Axis)



(e) Normal Stress acting on the Dam



(f) Equivalent (Von-Mises) Stress

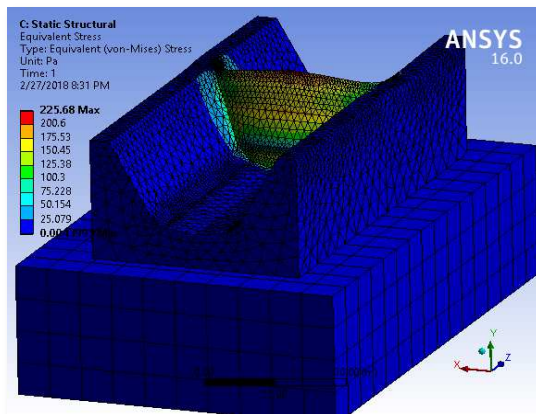
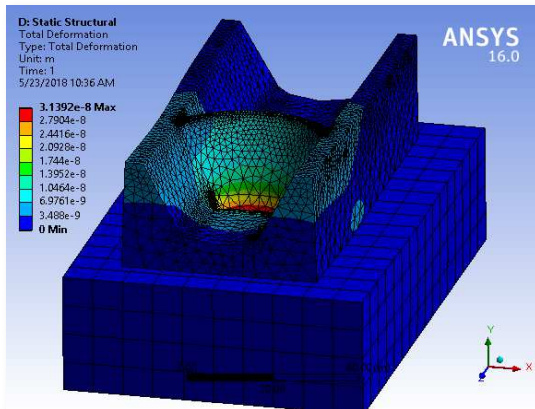
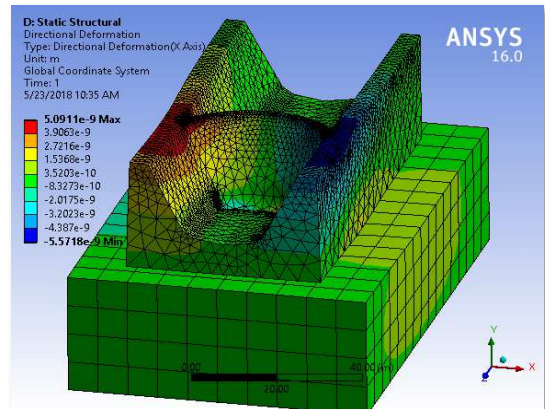


Fig. 17 Simulation of hydrodynamic forces occurring on the dam's upstream face

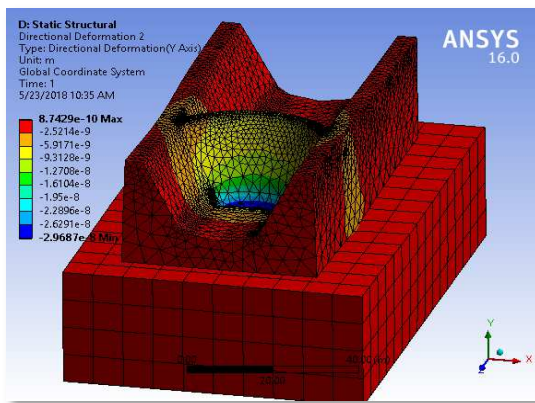
(a) Total Deformation of the dam



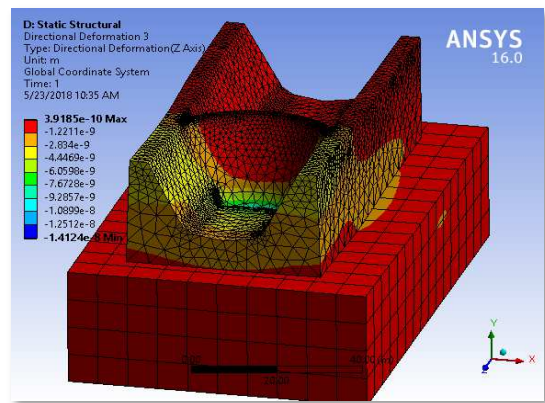
(b) Directional Deformation (X-Axis)



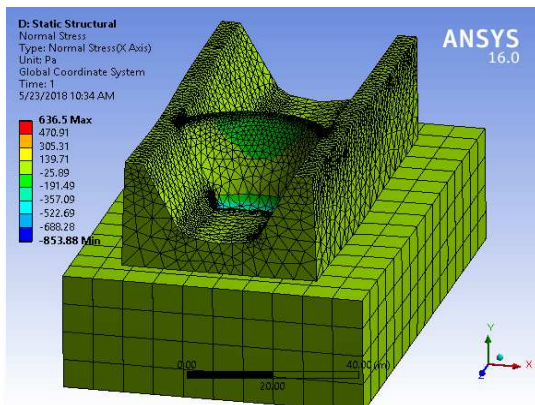
(c) Directional Deformation (Y-Axis)



(d) Directional Deformation (Z-Axis)



(e) Normal Stress acting on the Dam



(f) Equivalent (Von-Mises) Stress

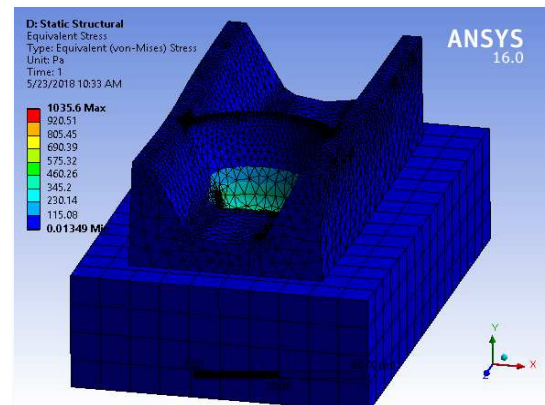
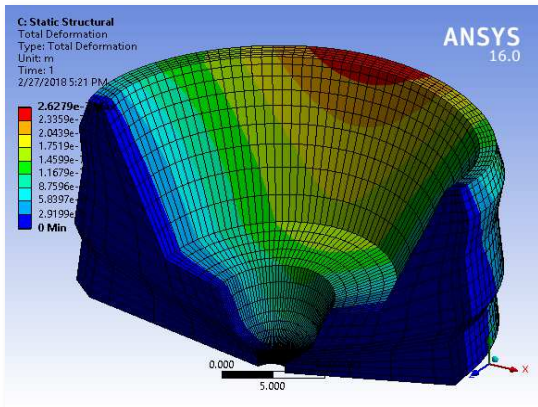
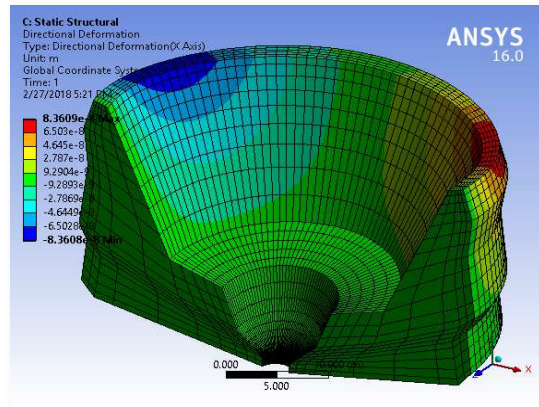


Fig. 18 Simulated horizontal inertia force on the dam's upstream face

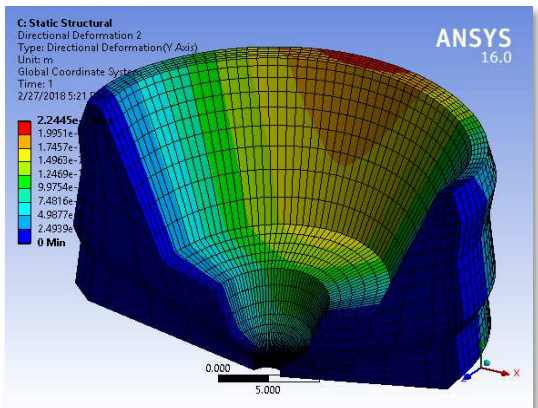
(a) Total Deformation of the dam



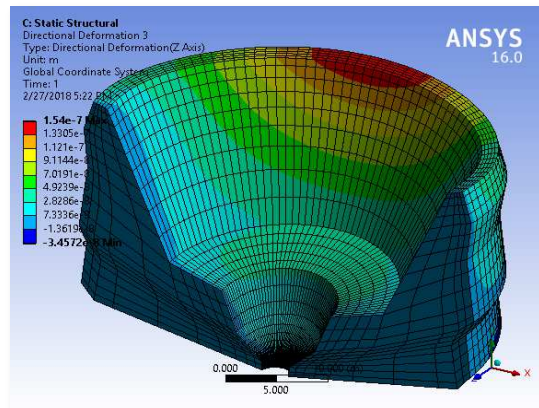
(b) Directional Deformation (X-Axis)



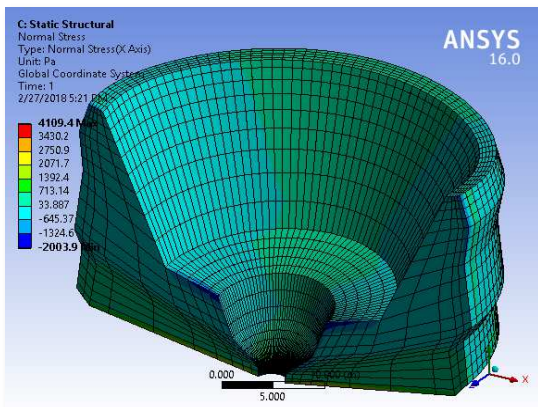
(c) Directional Deformation (Y-Axis)



(d) Directional Deformation (Z-Axis)



(e) Normal Stress acting on the Dam



(f) Equivalent (Von-Mises) Stress

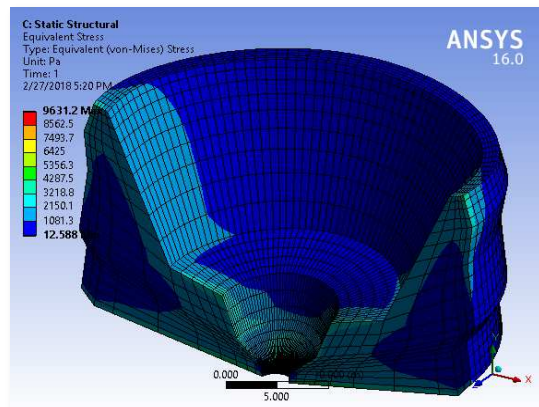
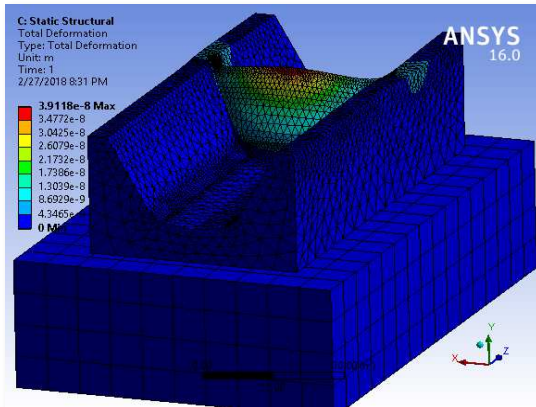
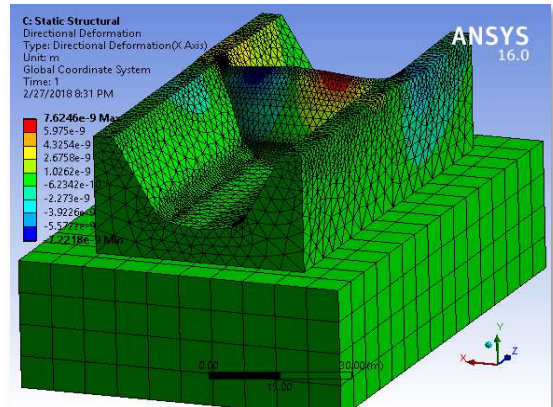


Fig. 19 Simulations of the effects of vertical earthquake stresses on the dam's bottom face

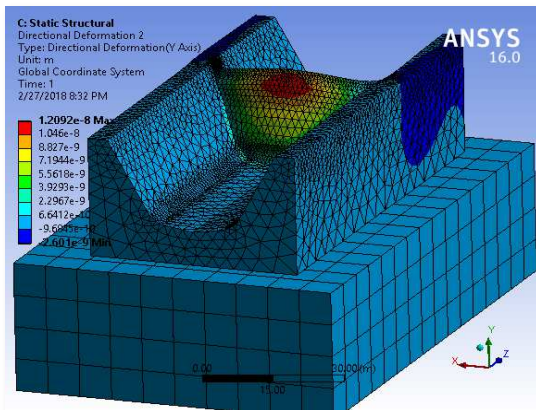
(a) Total Deformation of the dam



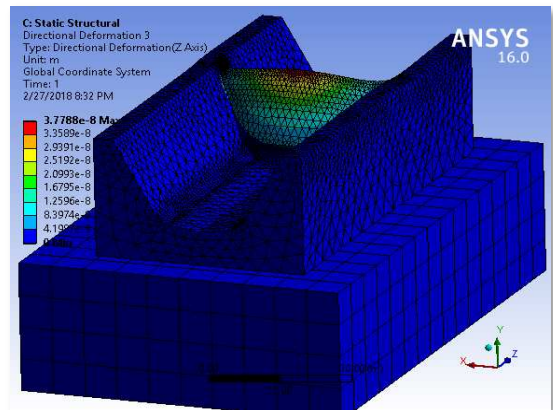
(b) Directional Deformation (X-Axis)



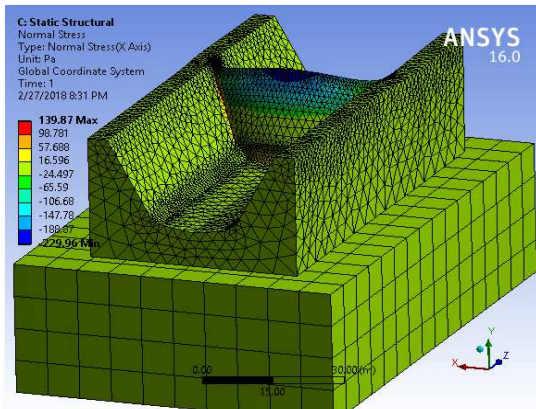
(c) Directional Deformation (Y-Axis)



(d) Directional Deformation (Z-Axis)



(e) Normal Stress acting on the Dam



(f) Equivalent (Von-Mises) Stress

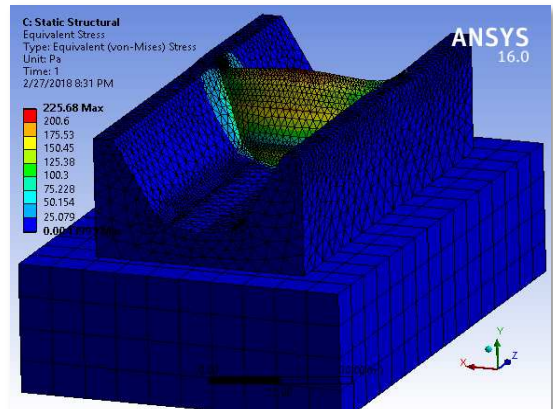
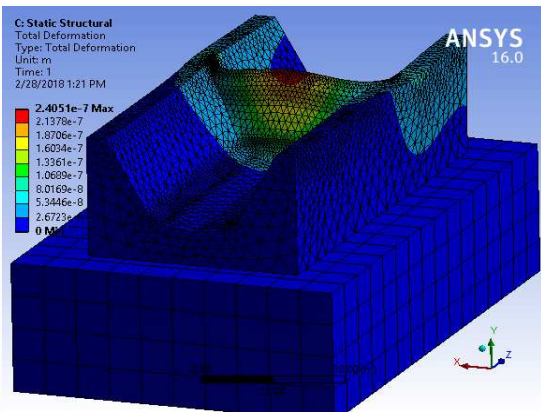
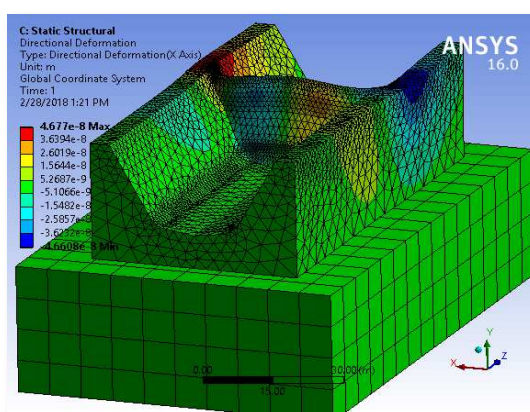


Fig. 20 Results of simulated vertical seismic forces occurring at the dam's bottom face

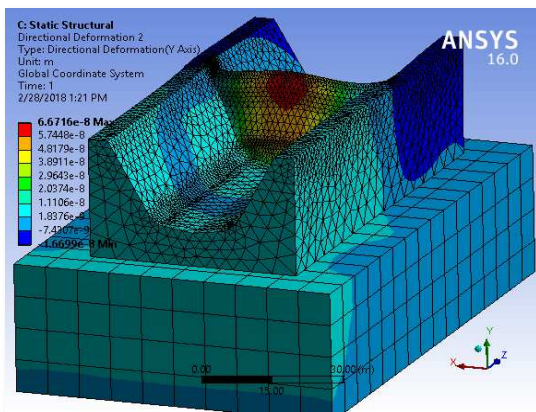
(a) Total Deformation of the dam



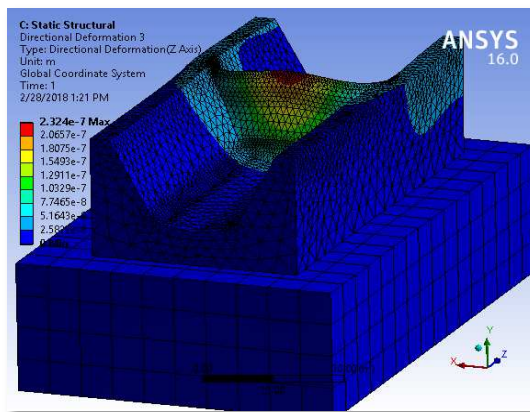
(b) Directional Deformation (X-Axis)



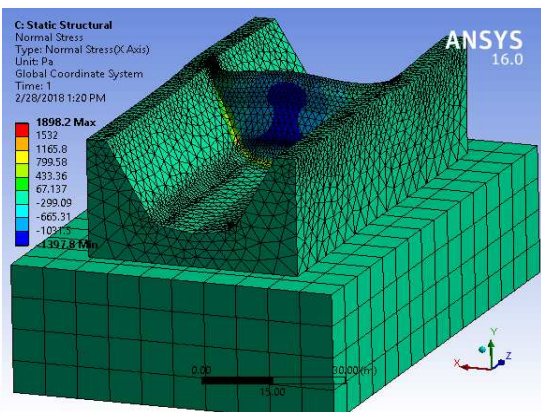
(c) Directional Deformation (Y-Axis)



(d) Directional Deformation (Z-Axis)



(e) Normal Stress acting on the Dam



(f) Equivalent (Von-Mises) Stress

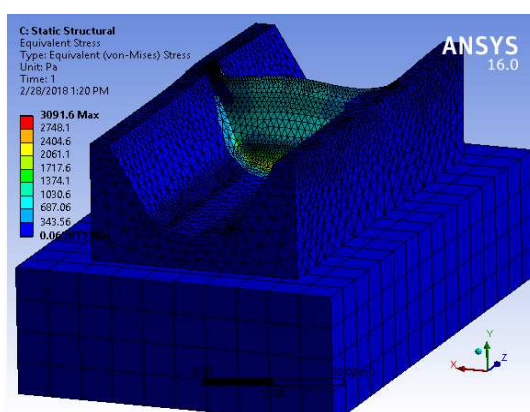


Fig. 21 Results of simulated wave pressure, horizontal inertia forces, and hydrodynamics on the upstream face of the arch dam

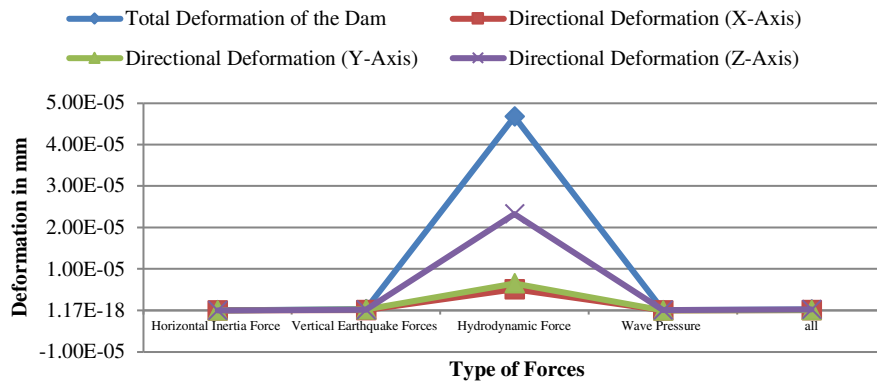


Fig. 22 Dam deformation due to various load cases

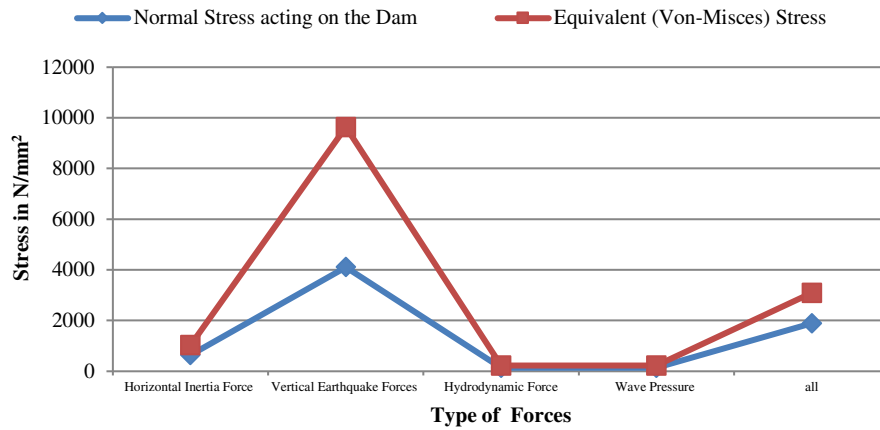


Fig. 23 Dam stress due to various load cases

As illustrated in Figs. 22 and 23, hydrodynamic forces acting on the dam are stronger than wave pressure, horizontal inertia forces, vertical earthquake acceleration, and semi-dynamic forces.

4. CONCLUSION

Dams, as all other structures, must be designed with extreme precision. The gravity dam portion must be the most cost-effective and meet all of the guidelines and specifications for stabilization. The purpose of this research is to determine the static response of an arch dam of various dam models. The effects of self-weight, static forces (vertical, horizontal, uplift, and silt pressure), and semi-dynamic forces (hydrodynamic forces, horizontal inertia forces, vertical acceleration, and wave pressure) are analysed for these models, and the summary of the result is presented.

The dam without a soil foundation deforms more than the dam with soil, but less than the dam with soil and reservoir. A dam with a soil foundation is under less stress than one without, but one with a soil and reservoir base is under much more stress.

Semi-dynamic forces (hydrodynamic and seismic forces) applied to the arch dam enhance deformation, normal stress, and equivalent (Von-Misses) stress compared to wave pressure, horizontal inertia forces, vertical earthquake acceleration, and comparatively exhibit greater values for hydrodynamic forces.

5. REFERENCES

- [1] Ali Rizwan, M.S. Hanumanthappa, Shyamli Paswan, A.K. Ghosh, and S.M. Govindan, Assessment of structural stability of an existing gravity dam using the finite element method and pseudo dynamic approach, Set Golden Jubilee Symposium, Indian Society of Earthquake Technology, Department of Earthquake Engineering Building IIT Roorkee, October 20-21, No. D009, 2012.
- [2] Zhuan-Yun, Static and dynamic analysis of high arch dam by three dimensional finite element methods, *Electronic Journal of Geotechnical Engineering*, Vol. 19, pp. 2537–2551, 2014.
- [3] V.P. Swapnal, and U.R. Awari, Effect of Soil Structure Interaction on Gravity Dam, *International Journal of Modern Trends in Engineering and Research (IJMTER)*, Vol. 2, No. 7, pp. 654–662, 2015.
- [4] D. Ajayakumar, K. Girija, and A. Raj, Static Analysis and Safety Evaluation of an Arch Dam, *International Journal of Innovative Research in Science, Engineering and Technology*, Vol. 4, No. 9, pp. 8369–8372, 2015. DOI:10.15680/IJIRSET.2015.0409051
- [5] R.P. Gupta, and M. Das, Dynamic Response Analysis of Middle Vaitarna Dam, Maharashtra, India-A Case Study, *International Journal of Emerging Technology and Advanced Engineering*, Vol. 9, No. 5, pp. 254–263, 2015.
- [6] Jiji Anna Varughese and Sreelakshmi Nikithan, Seismic behavior of concrete gravity dams, *Advances in Computational Design*, Vol. 1, No. 2, pp. 195-206, 2016.
<https://doi.org/10.12989/acd.2016.1.2.195>
- [7] Soumya, A.D. Pandey AD, R. Das, M.J. Mahesh, S. Anvesh, and P. Saini, Structural Analysis of a Historical Dam, *Procedia Engineering*, Elsevier B.V, Vol. 144, pp. 140–147, 2016.
<https://doi.org/10.1016/j.proeng.2016.05.017>
- [8] A. Margaret, K. Bennet, and K. Reni, Static Analysis of Gravity Dams Considering Foundation-Structure Interaction, *Applied Mechanics and Materials*, Vol. 857, pp. 237–242, 2017. <https://doi.org/10.4028/www.scientific.net/AMM.857.237>
- [9] Xin Zhong Zhang, Xiao Na Sun, Ke Dong Tang, Static and dynamic analysis of concrete gravity dams by ANSYS, *Applied Mechanics and Materials*, Vol. 438–439, pp. 1334–1337, 2015. <https://doi.org/10.4028/www.scientific.net/AMM.438-439.1334>
- [10] ANSYS. ANSYS User's Manual, *ANSYS Theory Manual*.
- [11] Sham Tickoo, *ANSYS- A Tutorial Approach by CAD/CIM Technologies*.